Nanoscale

PAPER

View Article Online
View Journal | View Issue

Cite this: *Nanoscale*, 2016, **8**, 2188

Luminescence quantum yields of gold nanoparticles varying with excitation wavelengths

Yuqing Cheng,[a] Guowei Lu,*[a,b,c] Yingbo He,[a] Hongming Shen,[a] Jingyi Zhao,[a] Keyu Xia[d] and Qihuang Gong[a,b,c]

Received 22nd October 2015,
Accepted 13th December 2015

DOI: 10.1039/c5nr07343j

www.rsc.org/nanoscale

Luminescence quantum yields (QYs) of gold nanoparticles including nanorods, nanobipyramids and nanospheres are measured elaborately at a single nanoparticle level with different excitation wavelengths. It is found that the QYs of the nanostructures are essentially dependent on the excitation wavelength. The QY is higher when the excitation wavelength is blue-detuned and close to the nanoparticles' surface plasmon resonance peak. A phenomenological model based on the plasmonic resonator concept is proposed to understand the experimental findings. The excitation wavelength dependent QY is attributed to the wavelength dependent coupling efficiency between the free electron oscillation and the intrinsic plasmon resonant radiative mode. These studies should contribute to the understanding of one-photon luminescence from metallic nanostructures and plasmonic surface enhanced spectroscopy.

Introduction

The novel optical properties of metallic nanostructures have attracted great interest in the past decade due to their potential applications in various fields such as biosensing, bioimaging, therapy of cancer labelling, *etc*. Light emission, *e.g.* photoluminescence (PL) from metallic nanostructures is a very interesting optical feature besides their widely known optical scattering and extinction properties. Compared with conventional organic fluorescent molecules presenting photoblinking and photobleaching, which limit their observation time inevitably, the PL from gold nanoparticles neither blinks nor bleaches. And the gold nanoparticles are nontoxic and biocompatible. It is of current interest to study the PL from robust nanostructures, that is, artificial molecules, such as gold nanoparticles. Mooradian has observed the PL spectra of bulk gold and copper excited with an argon laser in 1969.[1] Since his first observation of metal luminescence, numerous studies have reported this phenomenon by investigating metallic samples with different sizes and shapes such as rough surface films or nanoparticles.[2] The luminescence quantum yield (QY) of bulk gold is as low as on the order of 10^{-10}, while the gold nanostructures present luminescence QY to be several orders of magnitude higher than the bulk gold. Although the QY of gold nanoparticles is still several orders of magnitude lower than that of fluorescent organic dyes, their large absorption cross section compensates for their low QY, making them high-contrast imaging agents. Thus, the luminescence of gold nanoparticles has been successfully used in the imaging of cancer cells[3] and biosensing.[4]

The luminescence QY of the emitter is an important parameter to characterize its light emission properties. The early studies about the luminescence QY of gold nanoparticles have relied on ensemble measurements, and different QY values have been reported.[5] The QY of gold nanoparticles with diameters ranging from 5 to 80 nm has been reported to be about 10^{-7}–10^{-6} on average and be independent of size.[6,7] As for the gold nanorods with aspect ratios ranging from 2.0 to 5.4, the QY is about 10^{-4}–10^{-3} which is linearly dependent on the square of the nanorods' length.[8] While a recent detailed study of the luminescence from gold nanoparticles at the single nanoparticle level shows that the QY is different for different shapes and sizes. Especially, there is about an order of magnitude increase in QY for nanorods with longitudinal plasmon wavelengths longer than 650 nm compared to spheres.[9] Moreover, the PL QY of gold nanobipyramids was found to be twice higher than that of gold nanorods in a similar surface plasmon resonance range.[10] Besides, Stephan Link *et al.* investigated the strongly coupled 50 nm Au nanosphere dimers and found that the QY of the dimers is similar to the constituent monomers, which indicates that the enhanced local electric field of the dimer has little influence on its QY.[11] Other hybrid nanostructures have been studied. For instance, by defining

[a]*State Key Laboratory for Mesoscopic Physics, Collaborative Innovation Center of Quantum Matter, Department of Physics, Peking University, Beijing 100871, China. E-mail: guowei.lu@pku.edu.cn*
[b]*Collaborative Innovation Center of Quantum Matter, Beijing 100871, China*
[c]*Collaborative Innovation Center of Extreme Optics, Shanxi University, Taiyuan, Shanxi 030006, China*
[d]*ARC Centre for Engineered Quantum Systems, Department of Physics and Astronomy, Macquarie University, NSW 2109, Australia*

the dimensions of arrayed gold nanoparticles on a subwavelength-thin dielectric spacer and optically thick gold film which supports gap-surface plasmon resonances, Sebastian K. H. Andersen *et al.* have demonstrated the engineering of the spectral and polarization content of gold PL.[12] Besides the size and shape of the gold nanoparticles, the excitation laser wavelength may also influence the measured QY, and such a point of view has been mentioned in previous studies.[13] Recently, a detailed study by Fang *et al.* showed that the luminescence QY of gold nanorods for different aspect ratios were found to exponentially decrease as the energy difference between the excitation and emission wavelength increased.[14] However, there is not yet a direct verification in experiment by tuning the excitation wavelength to compare the PL QY of the same gold nanoparticles.

In this study, we explore the excitation wavelength dependence of the luminescence QY of gold nanoparticles including nanorods, nanospheres and nanobipyramids. The present study is performed at the single nanoparticle level by illuminating the same nanoparticles with 532 nm or 633 nm laser, respectively. The experimental results show that the QY of gold nanoparticles varies with the excitation wavelengths. Specifically, the QY becomes higher when the excitation wavelength is blue-detuned and closer to the nanoparticles' plasmon resonance band. The luminescence and scattering spectra of the same nanoparticle are correlated strongly which implies that the localized surface plasmon resonance (LSPR) dominates the observed light emission process. To understand the experimental findings, a phenomenological theoretical model based on the plasmonic resonator concept is implemented, and the theory explains well the excitation wavelength dependence of the QY. The wavelength-dependent coupling efficiency between the excitation light field driven free electron oscillation and the intrinsic LSPR mode results in the excitation wavelength dependence of the luminescence QY.

Results and discussion

For most molecular systems, the PL spectrum usually shows very little dependence on the excitation wavelength, and the luminescence QY also remains constant regardless of the excitation wavelength. There is a well-known Kasha–Vavilov rule which states that the luminescence QY is independent of the excitation wavelength, applying to a large variety of molecules. With very few exceptions, this rule holds true for most organic fluorescent molecules and artificial molecules such as semiconductor quantum dots. However, the applicability of a similar rule to the PL QY of the metallic nanostructures is rarely studied. In this study, we investigate the luminescence QY of single gold nanoparticles (with shapes of sphere, rod, and bipyramid) excited with 532 nm and 633 nm lasers systematically.

Single nanoparticle optical measurements were performed on a microspectroscopy system combining scattering, confocal scanning, and luminescence microscopy, assembled on an inverted optical microscope (NTEGRA Spectra, NT-MDT). The schematic of the setup and the experimental details about scattering, confocal scanning and photoluminescence are given in previous literature reports.[15,16] We further integrate a photothermal microscope based on the home-built microspectroscopy system to measure the photothermal signals of the single nanoparticles. The photothermal microscope has the irreplaceable advantage to detect the absorption of nanoparticles, especially the gold nanoparticles which have a prominent absorption cross section at the visible frequency range. Fig. 1 shows the schematic of the experimental setup about the photothermal microscope. Briefly, to obtain the photothermal signals, the continuous wave (CW) heating beam (532 nm or 633 nm laser) is modulated by an acoustic optical modulator (AOM, 23080-2-LTD, Gooch & Housego) at a frequency of 520 kHz. Circular polarization *via* a quarter-wave plate is utilized to average geometrical anisotropy of the gold nanoparticles. The power of the heating beams is ~0.16 mW. The probe beam overlapped with the heating beam is a 785 nm CW laser and the power is ~6.15 mW. Both heating and probe lasers are focused through a microscope objective (Olympus, numerical aperture 1.49) onto the sample. The energy absorbed by the nanoparticle is mainly released as heat giving rise to the "thermal lens" effect. The probe light which is scattered by the "thermal lens" is detected by the photodiode (PD, FPD510-FV, Thorlabs). The output from the photodiode was fed into a lock-in amplifier (HF2LI, Zurich Instruments), the lock-in amplifier demodulates the signal and provides the photothermal signal. And the photothermal images were recorded by raster scanning the sample. The confocal scanning image and photothermal scanning image are presented in Fig. 2(d) and (e), respectively.

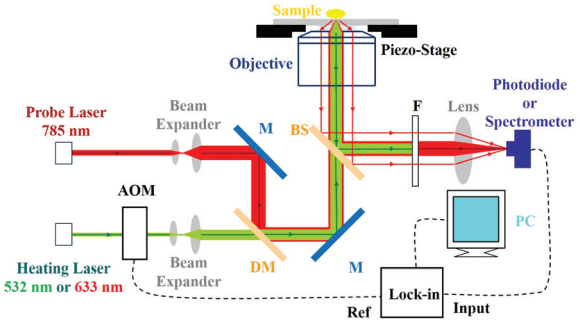

Fig. 1 Schematic of the experimental setup for photothermal, scattering and fluorescence microscopy. For photothermal microscopy, the probe laser and the heating laser are coaxially incident on the sample and the photodiode (PD) detects the photothermal signal. For fluorescence microscopy, the heating laser excites luminescence of the same sample. The white light is not shown in this scheme. AOM – acoustic optical modulator, M – mirror, DM – dichroic mirror, BS – beam splitter, F – filter.

To obtain the PL QY of a single nanoparticle, the PL spectrum and photothermal signals are necessary to calculate it quantitatively. When the gold nanoparticles are illuminated and detected under the same conditions, the luminescence

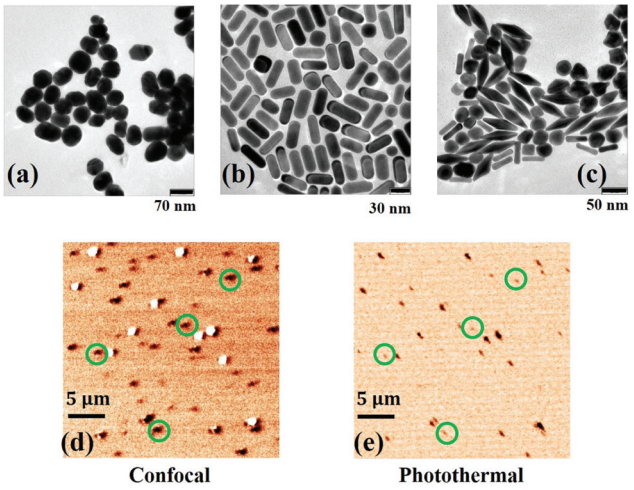

Fig. 2 (a), (b) and (c) are representative TEM images of the gold nanospheres, nanorods and nanobipyramids used in the experiments with scale bars of 70 nm, 30 nm and 50 nm, respectively. (d) Optical confocal scanning image in glycerol by the interference of the reflected and scattered light of the incident light acquired by using a photomultiplier tube (PMT) detector. (e) Photothermal scanning image by the photothermal signal acquired by using a photodiode detector with the same 30 μm × 30 μm scanning area.

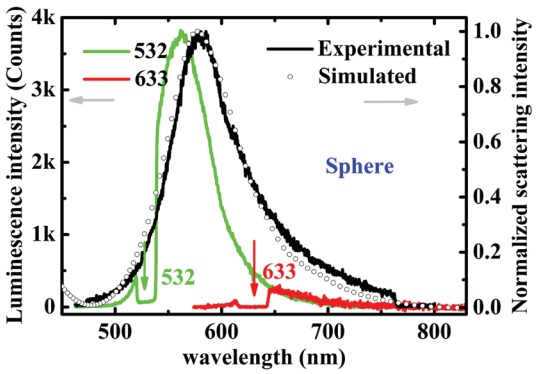

Fig. 3 Luminescence and normalized scattering spectra of the calibration reference gold nanosphere in glycerol. The luminescence spectra in green and red are excited with 532 nm and 633 nm laser, respectively. The black curve is the normalized scattering spectrum of the nanoparticle, and hollow circles are the calculated scattering spectrum of a gold nanosphere with 80 nm diameter in glycerol.

count-rate, $N_{\mathrm{em}} = \dfrac{N_{\mathrm{signal}}}{\Pi_{\mathrm{setup}}}$, indicates the number of emitted photons. While the number of absorbed photons, N_{abs}, is computed according to the absorption cross section (σ_{NR}) of the nanoparticle as $N_{\mathrm{abs}} = \dfrac{\sigma_{\mathrm{NR}} I_{\mathrm{exc}}}{\hbar\omega_{\mathrm{exc}}}$, where I_{exc} is the excitation heating laser intensity, and $\hbar\omega_{\mathrm{exc}}$ is the photon energy of the excitation light. The absorption cross section is proportional to the measured photothermal signal, written as: $\sigma_{\mathrm{NR}} = \sigma_{\mathrm{ref}} \times \dfrac{S_{\mathrm{NR}}}{S_{\mathrm{ref}}}$, where σ_{NR}, S_{NR}, σ_{ref} and S_{ref} are the absorption cross sections and the measured photothermal signals of the nanoparticles, and the reference calibration nano-objective. Finally, the luminescence QY is written as $\eta_{\mathrm{lum}} = \dfrac{N_{\mathrm{em}}}{N_{\mathrm{abs}}}$.

The representative TEM images of the gold nanospheres, nanorods and nanobipyramids used in the present study are shown in Fig. 2(a), (b) and (c), respectively. Firstly, the gold nanospheres with a diameter of 80 ± 10 nm used in this study were synthesized by the citrate reduction method. Although the ensemble extinction spectrum presents a single absorption band, there is an inhomogeneous distribution of size and shape leading to various LSPR bands of individual nanospheres.[17] To compare the luminescence QY of the gold nanoparticles with different shapes, we choose one of the measured gold nanospheres as a reference calibration sample. The scattering and PL spectra of this calibration nanoparticle are shown in Fig. 3, both of which are measured in glycerol. The scattering spectrum (black line) presents alike Lorentz line shapes, which implies a single plasmon resonant mode of the nanoparticle. Thus, we assume that the calibration reference nanoparticle is sphere shape approximately. Then a series of the scattering spectra of gold nanospheres with different diameters were calculated using the full 3D finite-difference time-domain (FDTD) method in glycerol to fit the experimental spectrum, and the diameter of the chosen nanoparticle was determined to be ~80 nm. After that, the calibration absorption cross sections of the gold nanoparticle are calculated to be 1.0×10^4 nm^2 at a wavelength of 532 nm and 4.0×10^3 nm^2 at a wavelength of 633 nm, which set a ground to compare the photothermal signal. As for the photoluminescence of the nanospheres, the power of the excitation light for the PL spectra and the photothermal measurements were set to the same level (~0.16 mW). We can see from Fig. 3 that the luminescence intensity of the nanoparticle excited with the 532 nm laser (green line) is much larger than that with the 633 nm laser (red line). Taking into account these data together, the luminescence QY of the nanoparticle was computed at different wavelengths, and we found that the QY of the nanospheres excited at 532 nm is about 3 times that excited at 633 nm. After calibrating the photothermal signals of different gold nanospheres using the reference sample, we can obtain the absorption cross section of each single nanoparticle, and then their luminescence QY.

Analogically, the luminescence QY of single gold nanorods can also be obtained in the same way. Fig. 4 shows the optical spectra of a representative single gold nanorod. The peak position of the spectra is around the wavelength of 680 nm due to the gold nanorod's longitudinal plasmon band, and the spectral shape of the PL follows approximately that of scattering. It should be noted that there is a slight difference between the PL and scattering, which could be related to the thermal equilibrium distribution of the sp-band electrons due to different light illumination conditions. The correlations between the PL and scattering spectroscopy allow us to distinguish single nanorods from aggregations and impurities.[13–15] For the luminescence and the photothermal measurements, the

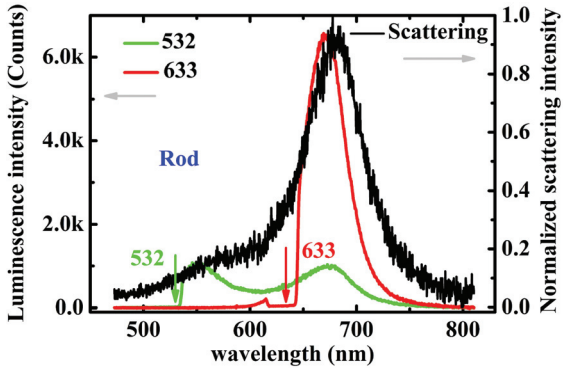

Fig. 4 Scattering (black line) and photoluminescence (green and red lines, excited with 532 nm and 633 nm laser, respectively) spectra of an individual gold nanorod in glycerol. The integrated time of both measurements is 10 s.

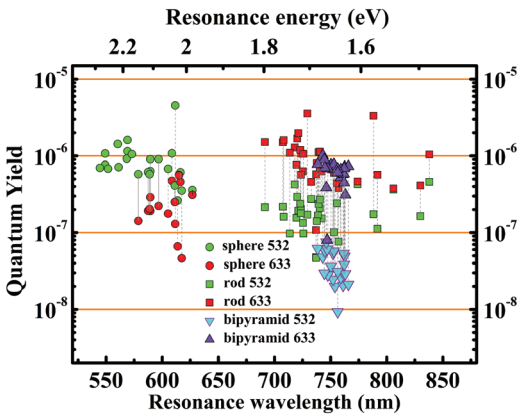

Fig. 5 Luminescence QY of the nanospheres (circles), nanorods (squares) and nanobipyramids (triangles) as a function of their plasmon resonance wavelengths in glycerol. Each pair of dots linked with vertical gray dash lines represent the same particle excited by different wavelengths. Green and red dots are for nanoparticles (spheres and rods) excited with circularly polarized 532 nm and 633 nm laser, respectively. Cyan and violet triangles are for nanobipyramids excited with circularly polarized 532 nm and 633 nm laser, respectively.

experimental conditions are the same as those implemented in the gold nanosphere cases. As seen from Fig. 4, it is obvious that the luminescence intensity of this nanorod excited by 633 nm is much larger than that excited by 532 nm. Employing the photothermal signals and the relationship of absorption cross section, we can obtain the absorption cross sections of the nanorod at 532 nm (3.17×10^3 nm^2) and 633 nm (2.26×10^4 nm^3). Then, the obtained QY of the nanorod excited at a wavelength of 633 nm is about 35 times that excited at 532 nm. In addition, the nanospheres with plasmon resonance around 550 nm were also measured and their QYs excited with the 532 nm laser are shown in Fig. 5 correspondingly. While, because of large blue-detune of the plasmon resonance band from the 633 nm excitation light, it is hard to detect the PL signal from these nanospheres when excited with the 633 nm laser. Hence, there are no QY data shown in Fig. 5 for the nanospheres with plasmon resonance around 550 nm.

Similarly, the PL spectra and the photothermal measurements were performed under the same conditions for the gold nanobipyramids. In Fig. 5, we summary that the measured QYs of 23 individual nanobipyramids as a function of their plasmon resonance wavelengths around 750 nm, 32 individual nanorods as a function of their plasmon resonance wavelengths ranging from 650 to 850 nm, and 25 individual nanospheres as the plasmon resonance wavelengths ranging from 540 to 620 nm. The QYs of the gold nanobipyramids are indicated by triangles, the squares for the gold nanorods, and the circles for the gold nanospheres. The QYs of the spheres and rods excited with the 532 nm laser are marked in green, and red symbols are for that excited with the 633 nm laser. For clarity, violet and cyan triangles indicate the bipyramids excited with 633 nm laser and 532 nm laser, respectively. Generally, the gold nanorods present higher luminescence QY than the gold nanospheres, which is in good agreement with a previous report.[9] Importantly, the experimental results doubtlessly show that the luminescence QY of gold nanoparticles is crucially dependent on excitation wavelengths. Specifically, the QY becomes higher when the excitation wavelength is blue-detuned and close to the nanoparticles' surface plasmon resonance band maximum.

In a previous study, the luminescence QY of the gold nanorods was found to be higher when the energy difference between the excitation and emission wavelength decreased.[14] These experimental results were explained based on the molecular system model qualitatively. While, as mentioned by the authors, this understanding is only a qualitative comparison, because multiphonon processes dominate the nonradiative relaxation in molecules. The detailed mechanism of the PL from the gold nanoparticles still remains an open question, for instance, plasmonic enhanced e–h recombination or plasmon emission is proposed to be responsible for the luminescence from the metallic nanostructures. We do not attempt to address this controversy, here, we present an alternate description of the light emission from the gold nanoparticle as a plasmonic resonator radiative decay process. This model would be helpful for us to understand the reason why the PL QY of gold nanoparticles is excitation wavelength dependent.

In a recent work, Xia *et al.* developed such a theoretical model to understand both Stokes and anti-Stokes light emission from a single gold nanorod.[18] The gold nanoparticle is treated as a plasmonic resonator due to the free electron collective oscillation. Fig. 6(a) shows the diagram of this model. The PL process from the metallic nanoparticles is described in three steps in the theory. First, the incident light field with the frequency of ω_{in} drives the sp-band free electrons of the nanorod to collectively oscillate at ω_{in}, which is called collective oscillation of free electrons that can scatter incident light elastically. Second, the partially created collective oscillation couples with the intrinsic LSPR mode $\hat{a}_c$ of the gold nanorod,

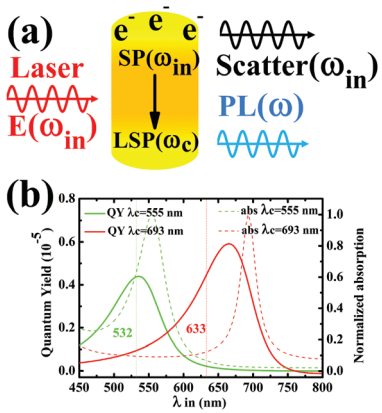

Fig. 6 (a) Diagram of the theoretical model for light emission from a single gold nanorod excited by a light field. (b) Solid curves stand for the theoretical QY of two individual nanoparticles with different resonance wavelengths (λ_c) as a function of the wavelength (λ_{in}) of an incident laser field. Dash curves display the calculated absorption spectra of the relevant nanoparticles. Vertical dot lines stand for emission light of 532 nm (green) and 633 nm (red).

described as the input α_{in} with the frequency of ω_c. Third, the LSPR mode radiation decays and couples to the free light field, and then generates the PL as an inelastic light emission, defined as an output α_{out} of the plasmon. Briefly, we write the input laser as $\alpha_{in} = E_{in}e^{-i\omega_{in}t}$, in case the electric field of the light is parallel to the LSPR mode. And the Hamiltonian of the LSPR mode of the gold nanoparticles can be described as:

$$H = \omega_c\hat{a}_c^{\dagger}\,\hat{a}_c + i\sqrt{2\kappa_{ex1}}(\alpha_{in}^{*}\hat{a}_c^{\dagger} - \alpha_{in}\hat{a}_c), \quad (1)$$

where ω_c is the resonance frequency of LSPR, $\hat{a}_c$ describes the LSPR mode and κ_{ex1} is the coupling rate between α_{in} and $\hat{a}_c$. Here the quantum average of the operator of excitation is replaced by a classical number, α_{in}, because the excitation laser includes enormous number of photons. The dynamics of the LSPR mode can be solved by the equation:[19]

$$\frac{\partial\hat{a}_c}{\partial t} = -(i\omega_c + \kappa)\hat{a}_c + \sqrt{2\kappa_{ex1}}E_{in}e^{-i\omega_{in}t}, \quad (2)$$

where κ is the total decay rate of the LSPR mode. The equation is solved to be

$$\hat{a}_c(t) = \hat{a}_c(0)e^{-(i\omega_c+\kappa)t} - \sqrt{2\kappa_{ex1}}\frac{E_{in}^{*}e^{-i\omega_{in}t}}{i(\omega_{in}-\omega_c)+\kappa} + \sqrt{2\kappa_{ex1}}\frac{E_{in}^{*}e^{-(i\omega_c+\kappa)t}}{i(\omega_{in}-\omega_c)+\kappa}. \quad (3)$$

Using the input–output relation $\langle\hat{a}_{out}\rangle = \sqrt{2\kappa_{ex2}}\hat{a}_c$,[20,21] where $\langle\hat{Q}\rangle$ is the quantum average of the operator Q and κ_{ex2} is the outgoing coupling rate, we obtain the light emission from the LSPR of the single gold nanorod as

$$I_{full}(\omega) = \Re\left[\int_0^{\infty}\lim_{t\to\infty}\hat{a}_{out}^{\dagger}(\tau+t)\hat{a}_{out}(t)e^{-i\omega\tau}d\tau\right]. \quad (4)$$

$I_{full}(\omega)$ includes PL $I_{PL}(\omega)$ and scattering $I_{SC}(\omega)$. After filtering the input laser field and using the quantum regression theorem, we obtain the PL intensity from $I_{full}(\omega)$ as

$$I_{PL}(\omega) = \frac{I_{in}A}{(\omega_c-\omega_{in})^2+\kappa^2}\frac{\kappa}{(\omega_c-\omega)^2+\kappa^2}, \quad (5)$$

where $I_{in} = |E_{in}|^2$ is the intensity of the input laser field, $A = 4\kappa_{ex1}\kappa_{ex2}$ is a scale coefficient. As we can see from the second term of equation, the PL spectrum is determined as a Lorentzian profile by this term and resembles the LSPR band when the excitation wavelength ω_{in} was fixed. While from the first term, we can conclude that the PL intensity increases as the detuning decreases between ω_{in} and ω_c, *i.e.*, the energy gap between the excitation wavelength and LSPR resonance wavelength as mentioned in previous work.[14] It should be noted that the light field driven free electron oscillation also directly radiates at the same frequency of ω_{in}, which is treated as resonant Rayleigh scattering term, and discussed in detail elsewhere.[18] For simplicity, based on the language of optical cavity, the plasmonic resonator can radiatively decay the absorbed energy. As a result, the spectral profile is determined by the mode. While the emission QY is related to the converse efficiency between the absorbed energy and the resonant radiative mode. That is to say that the coupling efficiency between the light field driven free electron oscillation and the intrinsic LSPR radiative mode of the gold nanorod determines the luminescence QY. This conclusion is reasonable and is consistent with the understandings based on the molecular system model which is enhanced by LSPR,[14] *i.e.*, the radiative rate is higher when the excited electrons are closer to the LSPR peak which results in a higher QY. Additionally, according to eqn (5), the PL intensity increases as the κ decreases which is related to the line width of the plasmon resonance band. Lower κ, *i.e.* less loss, usually results in a higher local field intensity. Thus, a stronger local field intensity around the plasmonic nanostructures often leads to higher PL intensities or quantum yields.

To demonstrate the change trend of luminescence QY as a function of the excitation wavelength, we calculate the integral spectrum from a boundary ω_{cut} to ω_b for the Stokes PL emission, where $\omega_b = \omega_{in} - \delta\omega$ is the deviation from ω_{in}. After obtaining the number of emitted photons, then, the QY can be evaluated as

$$\mathrm{QY}(\omega_{in}) = \frac{\left(\int_{\omega_{cut}}^{\omega_b}\frac{I_{PL}(\omega)}{\hbar\omega}d\omega\right)}{\left(\frac{I_{in}}{\hbar\omega_{in}}\right)} = \frac{A\omega_{in}}{(\omega_c-\omega_{in})^2+\kappa^2} \times\int_{\omega_{cut}}^{\omega_b}\frac{\kappa}{(\omega_c-\omega)^2+\kappa^2}\frac{1}{\omega}d\omega = \frac{A\omega_{in}}{(\omega_c-\omega_{in})^2+\kappa^2} \times\frac{1}{B^2}\left[\kappa\ln\left(\frac{\omega_{in}-\delta\omega}{\omega_{cut}}\sqrt{\frac{\kappa^2+(\omega_c-\omega_{cut})^2}{\kappa^2+(\omega_c-\omega_{in}+\delta\omega)^2}}\right) + \omega_c\left(\arctan\left(\frac{\omega_{in}-\delta\omega-\omega_c}{\kappa}\right)-\arctan\left(\frac{\omega_{cut}-\omega_c}{\kappa}\right)\right)\right], \quad (6)$$

where $B = \sqrt{\kappa^2 + \omega_c{}^2}$. On the basis of the formula, Fig. 6(b) shows the QY of two individual nanoparticles with different resonance frequencies as a function of the wavelength of the excitation laser. Here, ω_{cut} = 1.53 eV corresponding to a wavelength of 800 nm due to the PL spectrum range and $\omega_{in} - \delta\omega \approx 0.95\omega_{in}$ due to the blocking effect by the optical filters, which is consistent with the experimental conditions. It is clear that when the input laser frequency is blue-detuned and close to the resonance frequency of the nanoparticle, the QY reaches its maximum value. Therefore, we can intuitively figure out that the PL QY of the gold nanoparticles is excitation wavelength dependent. Specifically, in the present experimental study, for the gold nanospheres with plasmon resonance wavelengths ranging from 540 to 620 nm, the QY excited with the 532 nm laser is higher than that with the 633 nm laser. While for the gold nanorods with plasmon resonance wavelengths ranging from 650 to 850 nm, the QY excited by 633 nm laser is higher. Thus, this theoretical model provides us more understanding of the PL process from the metallic nanostructures. For the nanobipyramids, the PL QY in the present study was found to be almost equal to that of the nanorods in similar surface plasmon resonance, the result is not consistent with a previous report.[10] This implies that the QY of plasmonic nanoparticles could depend on other unknown factors such as the influence of the local environment or surfactants.

Conclusions

In summary, we demonstrate that the luminescence QYs of gold nanoparticles are excitation wavelength dependent in experiments. The photoluminescence of gold nanospheres, nanorods and nanobipyramids with different sizes and shapes was studied at the single nanoparticle level by illuminating with 532 nm or 633 nm laser, respectively. The experimental results show that the gold nanobipyramids and nanorods present higher luminescence QYs than the gold nanospheres being excited at a wavelength of 633 nm, while it reverses when the nanoparticles are illuminated at a wavelength of 532 nm. A phenomenological theoretical model based on the plasmonic resonator concept is implemented to explain well the excitation wavelength dependence of the QY. It was supposed that the coupling efficiency between the free electron oscillation driven by the excitation light and the intrinsic LSPR mode of the gold nanoparticles is responsible for the excitation wavelength dependent luminescence QY. These studies contribute to the understanding of one-photon luminescence from metallic nanostructures and plasmonic surface enhanced spectroscopy.[22,23]

Methods

Sample preparation

The colloidal gold nanospheres with a diameter of 80 ± 10 nm were synthesized by the citrate reduction method.[24] The gold nanorods and nanobipyramids are synthesized by the seed-mediated method.[25,26] The gold nanoparticles were immobilized onto silane functionalized glass coverslips in a manner similar to our previous report for gold nanospheres with an average interparticle spacing of several micrometers. Such an interparticle spacing is suitable for interrogation of isolated nanorods and nanobipyramids by the microspectroscopy system because the diffraction-limited spots are sufficiently separated so as not to overlap.

Optical measurements

A microspectroscopy system based on an inverted optical microscope (NTEGRA Spectra, NT-MDT) was developed to combine multifunctional optical measurements. The setup allows us to identify single isolated nanoparticles and *in situ* measure the photothermal signals, white light scattering spectra and luminescence spectra of the same nanoparticles. The experimental configurations were described in detail in the previous study.[15,16] Briefly, for the white light scattering spectrum measurements, a quasi-paralleled white light beam was approximately focused at the back focal plane of a numerical aperture 1.49, 60× TIRF oil-immersion objective lens (Olympus, Japan). The scattering spectrum was collected by using the same objective and directed into a spectrometer (NT-MDT, Russia).

Numerical simulation

The finite-difference time-domain (FDTD) method,[27] a powerful technique for metallic nanostructures with arbitrary geometries, is employed to calculate the optical responses. Absorption and scattering cross sections, near-field distribution and enhancement, and decay rates can be calculated with this method. The Drude–Lorentz dispersion model is used for the optical dielectrics of gold and the refractive indexes of the dielectric media are set to 1.49 for silica and 1.47 for glycerol, independent of frequency. In this article, we use the FDTD method to calculate the scattering cross sections of a gold nanosphere with glycerol as the environment media with a mesh grid of 1 nm.

Conflict of interest

The authors declare no competing financial interest.

Acknowledgements

This work was supported by the National Key Basic Research Program of China (grant no. 2013CB328703) and the National Natural Science Foundation of China (grant no. 61422502, 11374026, 91221304, 61521004, 11527901).

References

1 A. Mooradian, *Phys. Rev. Lett.*, 1969, **22**, 185–187.

2 G. T. Boyd, Z. H. Yu and Y. R. Shen, *Phys. Rev. B: Condens. Matter*, 1986, **33**, 7923–7936.
3 N. J. Durr, T. Larson, D. K. Smith, B. A. Korgel, K. Sokolov and A. Ben-Yakar, *Nano Lett.*, 2007, **7**, 941–945.
4 J. N. Anker, W. P. Hall, O. Lyandres, N. C. Shah, J. Zhao and R. P. Van Duyne, *Nat. Mater.*, 2008, **7**, 442–453.
5 J. N. Demas and G. A. Crosby, *J. Phys. Chem.*, 1971, **75**, 991–1024.
6 A. Gaiduk, M. Yorulmaz and M. Orrit, *ChemPhysChem*, 2011, **12**, 1536–1541.
7 E. Dulkeith, T. Niedereichholz, T. A. Klar, J. Feldmann, G. von Plessen, D. I. Gittins, K. S. Mayya and F. Caruso, *Phys. Rev. B: Condens. Matter*, 2004, **70**, 205424.
8 M. B. Mohamed, V. Volkov, S. Link and M. A. El-Sayed, *Chem. Phys. Lett.*, 2000, **317**, 517–523.
9 M. Yorulmaz, S. Khatua, P. Zijlstra, A. Gaiduk and M. Orrit, *Nano Lett.*, 2012, **12**, 4385–4391.
10 W. Rao, Q. Li, Y. Wang, T. Li and L. Wu, *ACS Nano*, 2015, **9**, 2783–2791.
11 D. Huang, C. P. Byers, L. Y. Wang, A. Hoggard, B. Hoener, S. Dominguez-Medina, S. Chen, W. S. Chang, C. F. Landes and S. Link, *ACS Nano*, 2015, **9**, 7072–7079.
12 S. K. H. Andersen, A. Pors and S. I. Bozhevolnyi, *ACS Photonics*, 2015, **2**, 432–438.
13 A. Tcherniak, S. Dominguez-Medina, W.-S. Chang, P. Swanglap, L. S. Slaughter, C. F. Landes and S. Link, *J. Phys. Chem. C*, 2011, **115**, 15938–15949.
14 Y. Fang, W.-S. Chang, B. Willingham, P. Swanglap, S. Dominguez-Medina and S. Link, *ACS Nano*, 2012, **6**, 7177–7184.
15 T. Zhang, H. Shen, G. Lu, J. Liu, Y. He, Y. Wang and Q. Gong, *Adv. Opt. Mater.*, 2013, **1**, 335–342.
16 G. Lu, L. Hou, T. Zhang, J. Liu, H. Shen, C. Luo and Q. Gong, *J. Phys. Chem. C*, 2012, **116**, 25509–25516.
17 Q. Wang, G. Lu, L. Hou, T. Zhang, C. Luo, H. Yang, G. Barbillon, F. H. Lei, C. A. Marquette, P. Perriat, O. Tillement, S. Roux, Q. Ouyang and Q. Gong, *Chem. Phys. Lett.*, 2011, **503**, 256–261.
18 K. Xia, Y. He, G. Lin, H. Shen, Y. Cheng, Q. Gong and G. Lu, 2015, arXiv:1407.6105.
19 K. Xia and J. Twamley, *Phys. Rev. X*, 2013, **3**, 031013.
20 M. J. Collett and C. W. Gardiner, *Phys. Rev. A*, 1984, **30**, 1386–1391.
21 C. W. Gardiner and M. J. Collett, *Phys. Rev. A*, 1985, **31**, 3761–3774.
22 K. Munechika, Y. Chen, A. F. Tillack, A. P. Kulkarni, I. Jen-La Plante, A. M. Munro and D. S. Ginger, *Nano Lett.*, 2011, **11**, 2725–2730.
23 C. Lumdee, B. Yun and P. G. Kik, *ACS Photonics*, 2014, **1**, 1224–1230.
24 G. Frens, *Nature Phys. Sci.*, 1973, **241**, 20–22.
25 B. Nikoobakht and M. A. El-Sayed, *Chem. Mater.*, 2003, **15**, 1957–1962.
26 M. Liu and P. Guyot-Sionnest, *J. Phys. Chem. B*, 2005, **109**, 22192–22200.
27 A. Taflove and S. C. Hagness, *Computational Electrodynamics*, Artech house, Boston, 2000.

